

EXPERIMENTAL CALIBRATION OF THE IP BEHAVIOR OF STRENGTHENED INFILL WALLS AND SEISMIC ANALYSIS INCLUDING IP/OOP EFFECTS

Marco Gaspari¹, Marco Donà¹, and Francesca da Porto¹

¹ University of Padova, Dept. of Geosciences
Via Gradenigo 6, 35131 Padova, Italy
e-mail: marco.gaspari.2@phd.unipd.it marco.dona.1@unipd.it, francesca.daporto@unipd.it

Abstract

Thin masonry infills, classified as nonstructural elements, and often neglected in design models, strongly influence the seismic behavior of RC frames by increasing the overall structural stiffness; in addition, they can be the cause of brittle failure mechanisms, such as soft-floor mechanisms. Moreover, given their very brittle behavior and high IP/OOP response interaction, they are easily damaged even at low to medium seismic intensities. As a result, they are responsible for the high loss of building functionality and high repair costs.

This paper presents several concentrated plasticity models for representing the IP behavior of different reinforced and unreinforced infills, calibrated for four different panels using experimental tests.

The objective is to provide simplified models, using a commercial FEA program, to best represent the nonlinear behavior of the infills. After IP calibration of the panels, the seismic analysis of an existing 6-story frame infilled with unreinforced and strengthened panels is presented. The conducted nonlinear dynamic analysis is aimed at estimating the expected annual loss (EAL), according to Italian guidelines, to evaluate the effectiveness of the adopted strengthening solution.

Keywords: masonry infill walls, In-Plane/Out-of-Plane seismic response; numerical models; experimental calibrations; infill strengthening solutions; expected annual loss.

1 INTRODUCTION

The use of clay masonry infill walls in reinforced concrete (RC) frames is a common construction practice worldwide. Despite the many experimental studies conducted to date on their seismic behavior, with a focus on their failure modes, the interaction with the RC frame, and the interaction between the in-plane (IP)/out-of-plane (OOP) behavior, they still represent a potential critical issue for the seismic performance of buildings. Indeed, they are generally classified as non-structural elements, and there are still no clear standard indications on their modeling/verification procedures; therefore, they are often overlooked in the design phase. In particular, thin masonry infills are characterized by very brittle behavior and high IP/OOP response interaction [1, 2, 3, 4, 5]. Hence, they are easily damaged even at medium-low seismic intensities and are consequently responsible for high losses in building functionality and high repair costs [6]. Various strengthening techniques have been investigated to reduce the vulnerability of these infills, some of which use textile or fiber-reinforced mortar solutions (TRM, FRM) [7, 8]. However, there is a lack of simplified models suitable for simulating the behavior of these strengthened panels, to conduct the necessary evaluations on the effectiveness of these solutions.

Therefore, this study proposes the calibration of the IP behavior of various thin masonry infill walls, both unreinforced and strengthened, based on previous experimental campaigns. The modeling and subsequent calibration of the infills were conducted with commercial FEA software, using the FEMA concentrated plasticity model [9]. In particular, four infill panels were considered: one unreinforced (URM) [1] and three strengthened, using a Fiber-reinforced plaster (F), a Fiber-reinforced plaster with Basalt mesh (FB), or a Render plaster with Basalt mesh and helicoidal Bars for connection to the upper beam (RBB) [7]. After IP calibration of the panels, the seismic analysis of an existing 6-story case study frame, in-filled with both URM and RBB panels, is presented. The conducted analysis, which is non-linear dynamic, is addressed to the estimation of the expected annual loss (EAL), according to the Italian guidelines [10], to evaluate the effectiveness of the adopted strengthening solution. The verification of the reduced OOP capacity of the panels is performed a posteriori, based on the recorded inter-story drift and appropriate degradation laws [11], and is considered in the estimation of the EAL. The results demonstrate the importance of considering the IP effects of the panels, albeit in a simplistic way, as well as the effectiveness of the RBB strengthening solution.

2 CALIBRATION OF THE IP BEHAVIOR THROUGH TEST RESULT

2.1 Presentation of the reference tests

The experimental results, used for calibration, concern four types of thin panels with horizontal holes tested both in-plane and out-of-plane by Calvi and Bolognini [1] at the University of Pavia (UniPV) and by Minotto et al. [7] at the University of Padua (UniPD). Thin walls made of clay units with horizontal holes have been the typical lightweight envelope system used since the 1960s and are very common in existing buildings.

Both experimental campaigns use wall panels with similar lengths, heights, and thicknesses. The characteristics of the experimental sets and the main results are shown in Table 1, Figure 1, and Figure 2, respectively.

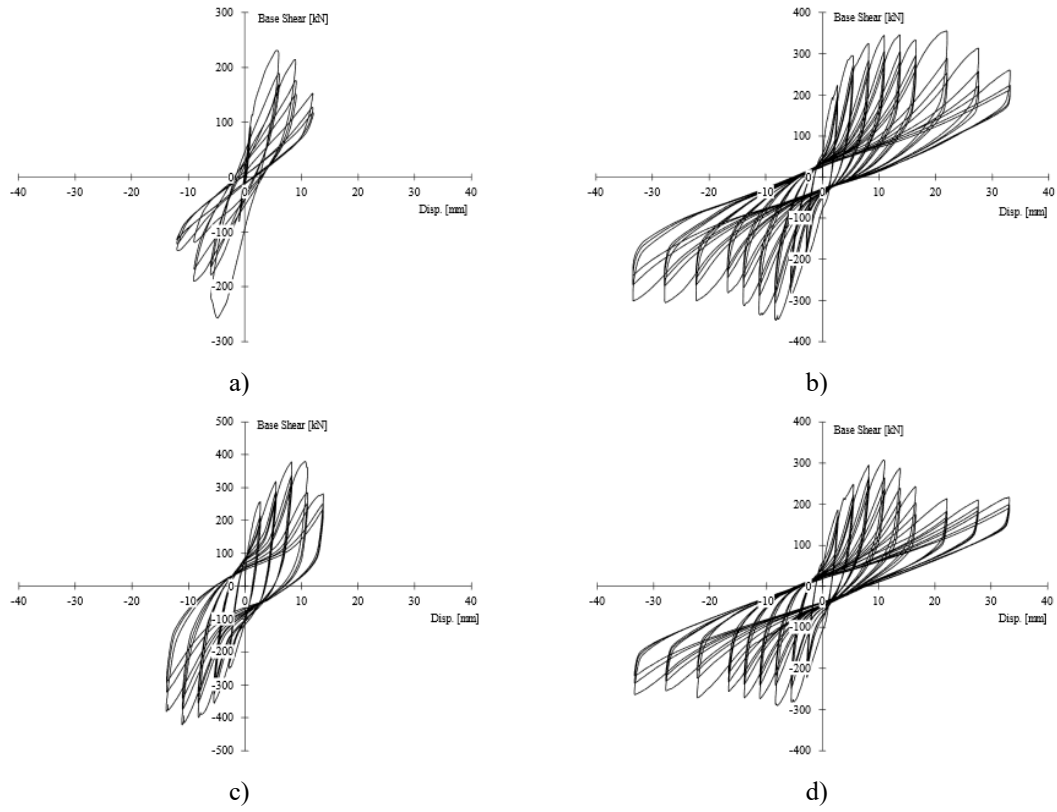


Figure 1: IP hysteretic cycles of infilled frames type URM (a), F (b), FB (c), and RBB (d)

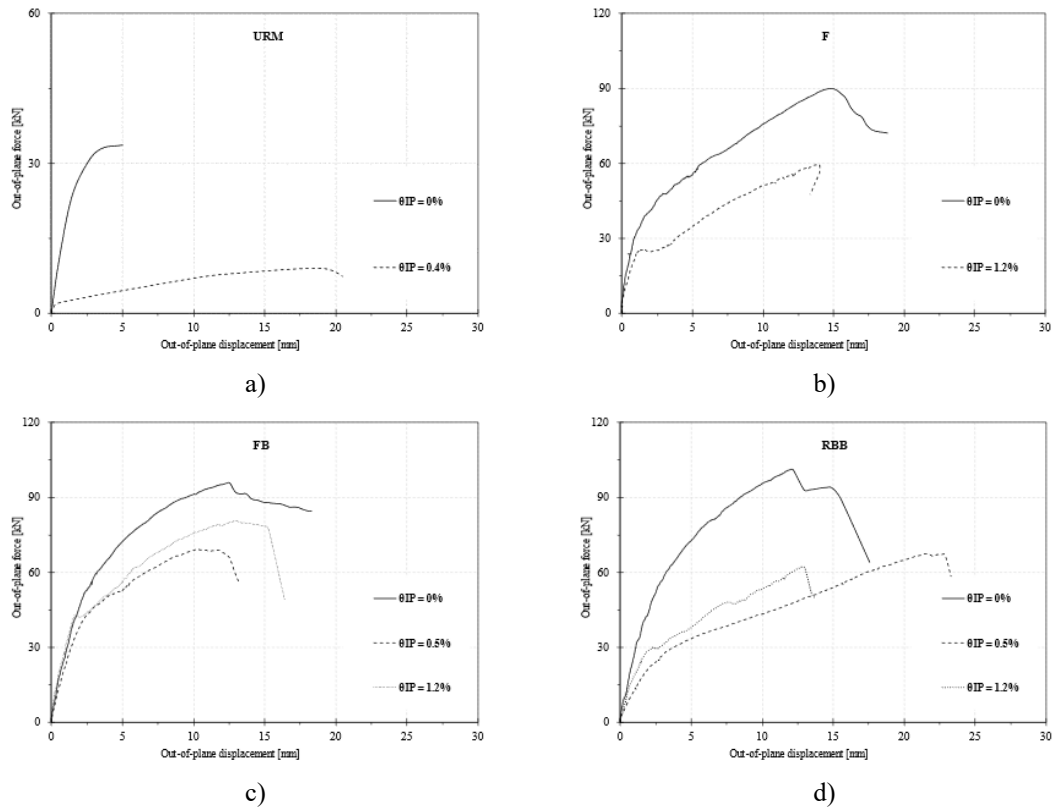


Figure 2: OOP force-displacement curves of infilled frames type URM (a), F (b), FB (c), and RBB (d)

		UniPV [1]	UniPD [7]		
		URM	F	FB	RBB
RC frame	Column section [mm]	300 x 300		300 x 300	
	Beam section [mm]	250 x 500		250 x 500	
	Frame height [mm]	3250		3200	
	Frame length [mm]	4800		4750	
	Concrete compressive strength [MPa]	30		30	
	Concrete elastic modulus [MPa]	25000		25000	
	Steel yield strength [MPa]	560		450	
	Steel elastic modulus [MPa]	195000		200000	
Masonry infill	Length L_w [mm]	4200		4150	
	Height h_w [mm]	2750		2650	
	Thickens t_w [mm]	115 (+ 20 mm plaster)		120 (+30 mm plaster)	
	Masonry units [mm]	245 x 245 x 115		250 x 250 x 120	
	Compressive strength f_m [MPa]	1.1	2.8	2.8	2.9
	Elastic modulus E_m [MPa]	1873	4752	4752	4777

Table 1: Geometry and material properties for the infilled RC frames tested.

2.2 Presentation of the FEMA model for inelastic hinge

In the proposed calibrations (see Figure 3), implemented through MidasGen [12] FEA software, the reinforced concrete frame was modeled using beam-column elements with non-linear fiber sections. The Kent-Scott-Park [13] constitutive law was considered for confined and unconfined concrete, while the steel bars used elastoplastic behavior with strain hardening, as proposed by Menegotto & Pinto [14]. The material laws, derived from the design features of the experimental tests (see Table 1), were calibrated to best fit the experimental results. The infill panels were modeled by two equivalent struts for each diagonal, each of which is defined by a truss element with concentrated plasticity defined according to FEMA [9]. The dimensions assumed to represent the diagonal strut are the effective thickness t_w of the panel, and its equivalent width w (see Figure 3), calculated according to Mainstone RJ. [15], and the contact length (l_c) defined according to Smith BS [16]. Table 2 shows all the geometric parameters of the struts elements, and thus in addition to w and l_c , the thickness (t_w), the equivalent area (A_{eq}), the stress centroid in the opposite column $y_c = l_c/3$, under the assumption of triangular stress distribution [17]. For more details on the calculation of these parameters, including the estimation of the inclined strut model (E_w), see Donà et al. [18]. It is useful to consider that these values refer to the equivalent diagonal strut, so the two trusses have $w/2$ and $A_{eq}/2$.

The results of the model calibration, for all experimental campaigns, are reported in Table 3 and Figure 4, respectively for the main parameters of the proposed models and the representation of the force-deformation. Comparisons between the experimental campaigns and calibrated FEMA models are shown in Figure 5.

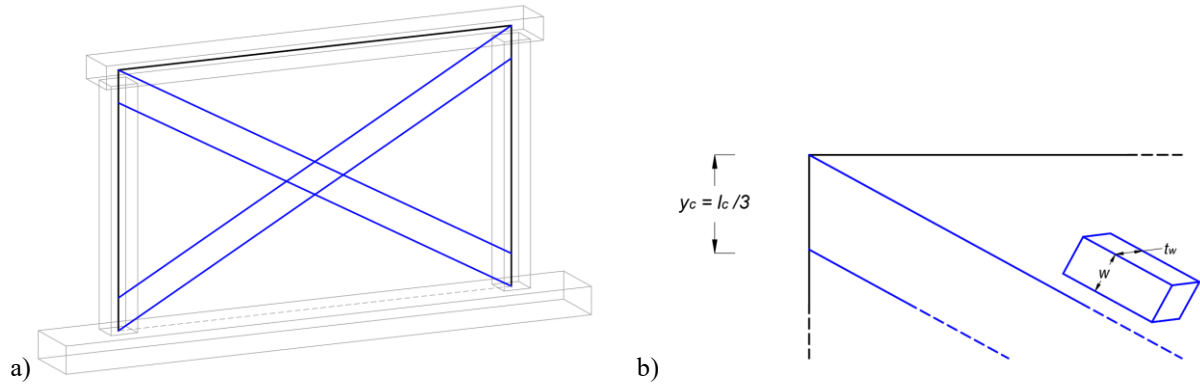


Figure 3: Scheme of the infilled frame model used (a), detail of the contact length (b)

Type of infill	t_w [mm]	w [mm]	A_{eq} [mm ²]	l_c [mm]	y_c [mm]	E_w [MPa]
URM	115	529.79	60926	1105	368	9000
F		529.25	63509	1114	371	8100
FB	120	512.37	61484	1027	342	11200
RBB		506.31	60757	998	332	12615

Table 2: Parameter of the equivalent strut

	URM		F		FB		RBB	
	F/F_y	D/D_y	F/F_y	D/D_y	F/F_y	D/D_y	F/F_y	D/D_y
-E	-0.4	-8	-0.65	-6.5	-0.4	-9	-0.4	-10
-D	-0.4	-4	-0.65	-6	-0.4	-8.5	-0.4	-9
-C	-1.1	-1.2	-1.3	-4	-1.5	-3	-1.05	-5.5
-B	-1	-1	-1	-1	-1	-1	-1	-1
A	0	0	0	0	0	0	0	0
B	1	1	1	1	1	1	1	1
C	1.06	6	1.06	6	1.06	6	1.06	6
D	1.05	6.3	1.05	6.3	1.05	6.3	1.05	6.3
E	1.05	8	1.05	8	1.05	8	1.05	8
Compression Yield Strength F_y [kN] (+)	120		140		125		130	
Tensile Yield Stress F_y [kN] (-)	0.001		0.001		0.001		0.001	
Exponent in Un- loading Stiffness	1.00		0.01		0.01		0.15	
Pinching-Rule Factor	1.00		1.0		0.5		0.5	

Table 3: FEMA model parameters calibrated on the experimental test and normalized on the yield strength.

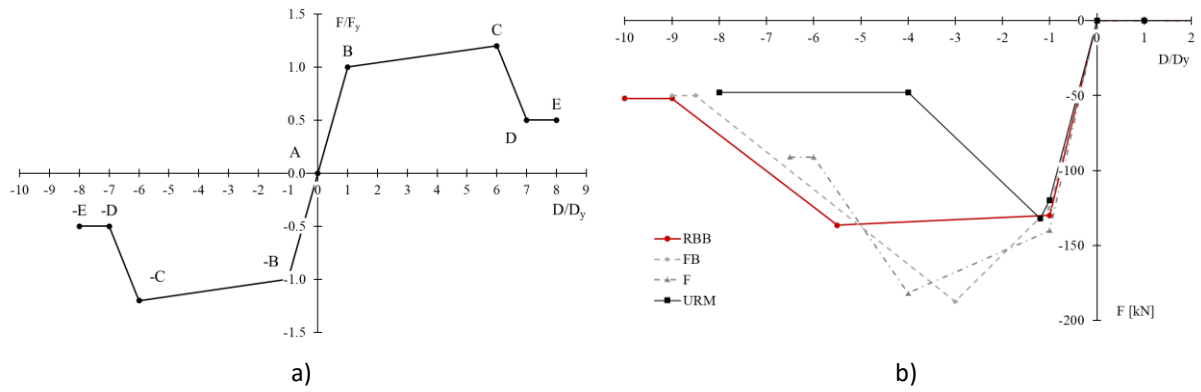


Figure 4: Figure 4: Property of the inelastic hinge a) FEMA model teoric, b) calibrated FEMA models

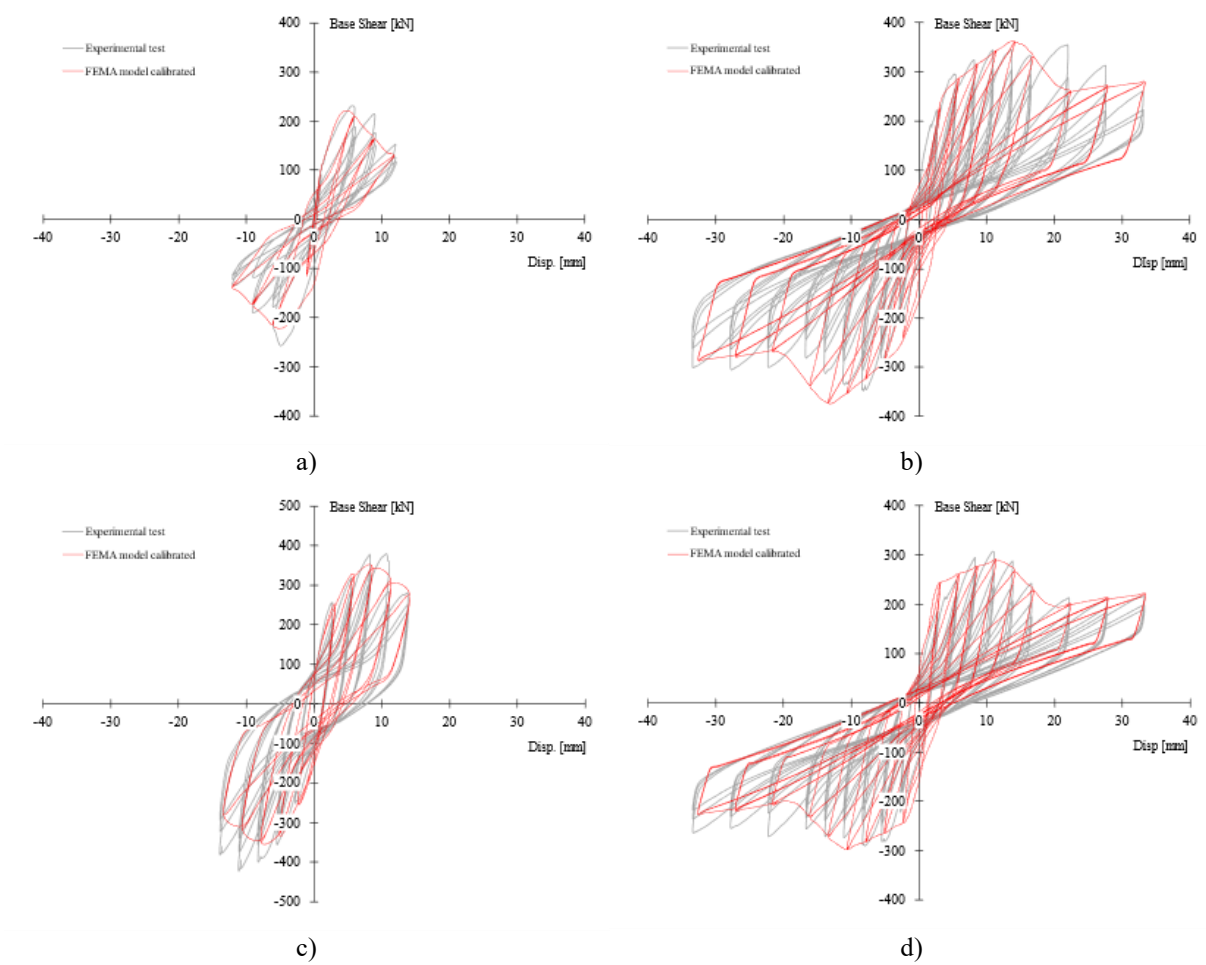


Figure 5: Result of the calibration with the FEMA model; URM (a), F (b), FB (c), and RBB (d)

3 SEISMIC ANALYSIS OF AN EXISTING 6-STORY RC FRAME BUILDING

To investigate the effects of infill walls on the seismic behavior of reinforced concrete (RC) structures, the previous calibrated infill models were adopted in an RC frame model representative of Italian buildings designed for gravity load only. In particular, the unreinforced infills (URM) and the strengthened infills RBB were selected for this calculation example.

The case study structure is ideal, and assumed to be in L'Aquila, Italy. This building has 6 stories, with a story height of 2.80 m for the first story and 2.90 m for the subsequent ones. The plan configuration is regular, with 4 bays in one direction and 2 in the orthogonal one. The load-bearing structure consists of RC beams and columns, with the latter having a spacing of 4.5 m in both directions. The floors are arranged along the short direction of the structure.

The average compressive strength of concrete used in the model is $f_{cm} = 23.46$ MPa and the yield strength of steel is $f_{ym} = 369.9$ MPa. The characteristics of the cross-sections of columns and beams are given in Table 4, while the loads to the structure are given in Table 5.

A linear dynamic analysis was carried out on the bare frame models, as a reference, and then a nonlinear dynamic analysis on the infilled frame, considering both infill URM and RBB (see Figure 6). The linear dynamic analysis was realized with the spectrum of the city of L'Aquila, according to the Italian [19], [20] codes, while 8 spectrum-compatible accelerograms of L'Aquila were used for the nonlinear analysis.

		Section [cm]	Long. Reinforcement [mm]	Ties / Stirrups [mm]
1° and 2° stories	Column	30 x 30	4 ϕ 16	
	Corner column	25 x 25	4 ϕ 12	ϕ 6/20 cm
	Beam	70 x 24	8/10 ϕ 16	
3° and 4° stories	Column	30 x 30	4 ϕ 16	
	Corner column	25 x 25	4 ϕ 12	ϕ 6/20 cm
	Beam	70 x 24	8/10 ϕ 16	
5° story	Column	30 x 30	4 ϕ 16	
	Corner column	25 x 25	4 ϕ 12	ϕ 6/20 cm
	Beam	70 x 24	8/10 ϕ 16	
6° story	Column	30 x 30	4 ϕ 16	
	Corner column	25 x 25	4 ϕ 12	ϕ 6/20 cm

Table 4: Sections and reinforcement details of the R.C. elements of the case study analyzed

	Interstory floor	Roof floor
Structural dead load (G1) [kN/m ²]	3.11	3.11
Non-structural dead load (G2) [kN/m ²]	2.45	2.05
Live load (Q) [kN/m ²]	2.00	0.90

Table 5: Loads to the building

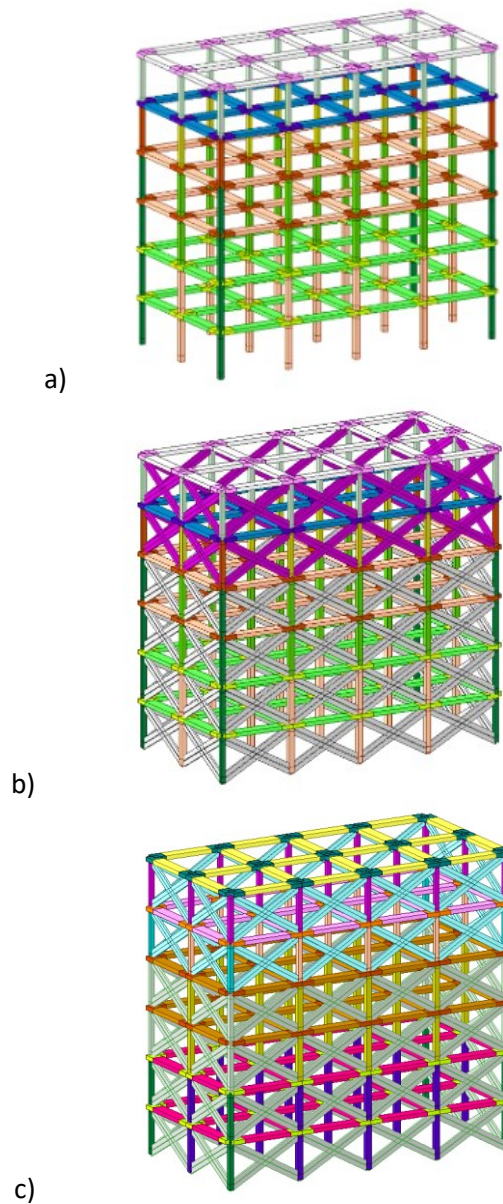


Figure 6: FEM model of the bare frame building (a), with the URM infill walls (b) and with RBB infill walls (c)

The behavior of the structure with the two different infills was done through the evaluation of the building's Risk Class according to the Italian Seismic Classification procedure [10]. Two parameters are necessary for the calculation of the Risk Class. The first is the expected average annual loss (shortly named EAL), which considers the economic losses associated with the damage of structural and non-structural elements and related to the reconstruction cost (CR) of the building neglecting its contents. The reconstruction costs are defined in the following Table 6.

Limit State	IDL	OLS	DLS	ULS	CLS	RLS
CR [%]	0	7	15	50	80	100

Note: IDL=Initial Damage Limit State; OLS=Operational Limit State; DLS=Damage Limit State; ULS=Ultimate Limit State; CLS=Collapse Limit State; RLS=Reconstruction Limit State.

Table 6: Building reconstruction cost at each Limit State

The second parameter is the safety index at the Ultimate Limit State (IS-V) defined as the ratio between the capacity and demand in terms of PGA at the Ultimate Limit State. The IS-V safety index is better known as Risk Index. The procedure for the calculation of the PAM index follows the next steps.

1. Execution of the numerical analyses and evaluation of the capacity in terms of PGA at DLS and ULS. For the following analyses, the DLS was assumed as the DLS whereas the ULS was the ULS.
2. Calculation of the capacity return period corresponding to each Limit State as follows.

$$T_{rC} = T_{rD} \left(\frac{PGA_C}{PGA_D} \right)^\eta \quad (1)$$

where T_{rC} is the return period of the capacity, T_{rD} is the return period of the demand, PGA_C and PGA_D are the capacity and the demand respectively, and η a coefficient which is a function of ag . In a simplified way it can be assumed as $1/0.49$.

Calculation of the annual average frequency of exceedance λ at each Limit State is defined in Table 5. The capacity corresponding to the Operational and Collapse Limit States was assumed in a simplified way as $\lambda_{OLS} = 1.67\lambda_{DLS}$ e $\lambda_{CLS} = 0.49\lambda_{ULS}$. In addition, the Reconstruction Limit State has the same T_r as the CLS and the Initial Damage Limit State occurs for a return period of 10 years. Associating each Reconstruction Cost to the corresponding λ at each Limit State it is possible to define a linear piecewise function and the area under the curve represents the EAL index.

3. Calculation of the IS-V index as the ratio between the capacity and the demand at ULS.
4. Definition of the EAL and IS-V classes according to the following Table 6 and Table 7.
5. The building Risk Class is defined as the worst condition between EAL and IS-V classes.

<i>EAL index</i>	<i>EAL class</i>
$EAL \leq 0.50\%$	A_{EAL}^+
$0.50\% < EAL \leq 1.00\%$	A_{EAL}
$1.00\% < EAL \leq 1.50\%$	B_{EAL}
$1.50\% < EAL \leq 2.50\%$	C_{EAL}
$2.50\% < EAL \leq 3.50\%$	D_{EAL}
$3.50\% < EAL \leq 4.50\%$	E_{EAL}
$4.50\% < EAL \leq 7.50\%$	F_{EAL}
$7.50\% \leq EAL$	G_{EAL}

Table 7: EAL classes

<i>IS-V index</i>	<i>IS-V class</i>
$IS-V \geq 100\%$	A_{IS-V}^+
$80\% \leq IS-V < 100\%$	A_{IS-V}
$60\% \leq IS-V < 80\%$	B_{IS-V}
$45\% \leq IS-V < 60\%$	C_{IS-V}
$30\% \leq IS-V < 45\%$	D_{IS-V}
$15\% \leq IS-V < 30\%$	E_{IS-V}
$IS-V \leq 15\%$	F_{IS-V}

Table 8: IS-V classes

The capacity PGA was obtained iteratively by scaling the set of accelerograms until the relevant Limit State was reached. The criteria shown adopted for this purpose are given in Table 9. OOP verification of the infills was done retrospectively as specified by EC6 [21], calculating the initial capacity of URM infills according to EC6 [21] and RBB infills as specified by Hak er all. [22], then reducing it as a function using the IP/OOP degradation law of Minotto et all. [7].

<i>Limit States</i>	<i>Performance levels</i>
<i>DLS</i>	$\min \{ \theta_{IP}=0.3\%; \text{column yielding} \}$
<i>ULS 1</i>	flexural failure
<i>ULS 2</i>	$\min \{ \text{flexural failure; OOP infill failure} \}$
<i>ULS 3</i>	$\min \{ \text{flexural failure; shear failure; OOP infill failure} \}$

Table 9: Definition of performance levels for achieving damage limit states and ultimate

3.1 Comparison of the building Risk Class

Figure 7 shows the EAL curves calculated for the structure infilled with URM and RBB infill for the different performance levels shown in Table 9. The DLS for both types of infill is always reached by column yielding, while the ULS is reached by either infill ejection or column flexural failure for URM and RBB infill, respectively. By performing column shear verification, the ultimate limit state is reached earlier for both types of infill.

For completeness, Table 10 shows the values of the EAL and IS-V parameters required for seismic class calculation. The bare frame results in the case with the lowest seismic class (*E*), this is due to the large deformability of the frame, the addition of the infills leads to a general improvement in behavior, reaching the seismic class of level *B* for the RBB infill. Considering the shear failure of the columns worsens the situation for both infills, lowering the class of the building infilled with the RBBs. Therefore, it is important to consider combined interventions on the panels and on the columns/shear nodes to optimize the results.

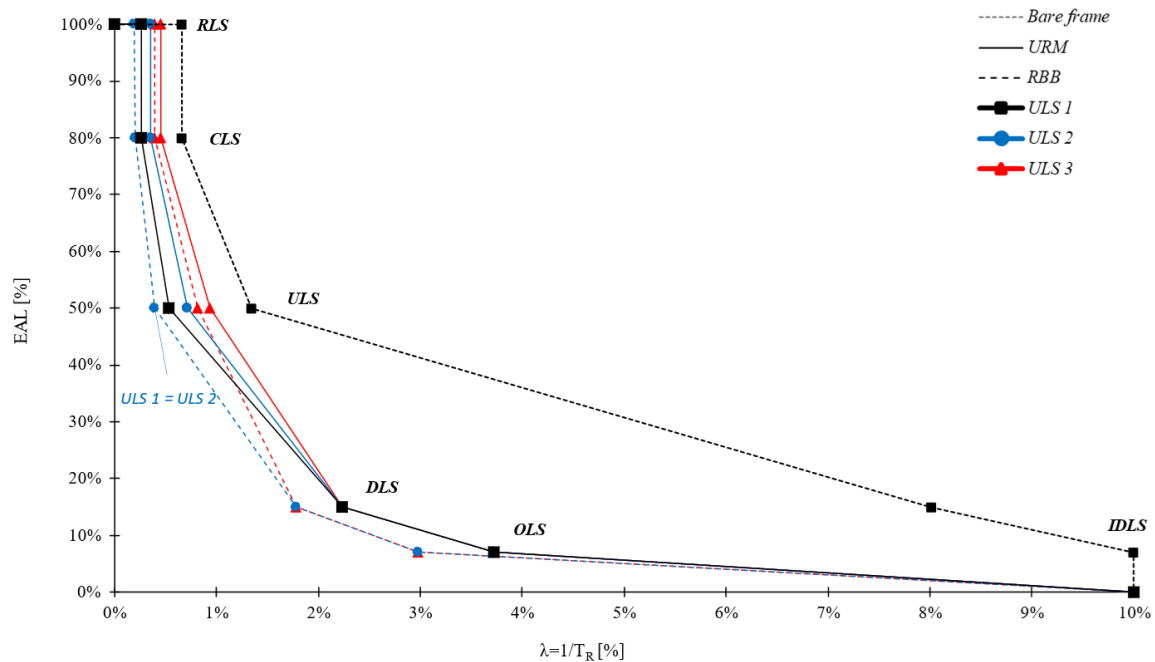


Figure 7: Comparison of the expected annual loss

		<i>Seismic risk classification</i>				
	<i>Type of failure</i>	<i>Expected annual loss (EAL) [%]</i>	<i>EAL Class</i>	<i>Security Index [%]</i>	<i>IS-V Class</i>	<i>Seismic class</i>
<i>Bare Frame</i>	<i>Flexural failure</i>	3.75	E	40.32	D	E
<i>URM</i>	<i>OOP infill</i>	1.47	B	54.78	C	C
	<i>Shear failure</i>	1.57	C	48.14	C	C
<i>RBB</i>	<i>Flexural failure</i>	1.16	B	73.04	B	B
	<i>Shear failure</i>	1.36	B	51.46	C	C

Table 10: Comparison of the seismic risk of the case study

4 CONCLUSION

This paper presents different FEMA concentrated plastic hinges within commercial FEA software. These infill models were calibrated on four different thin infills, one unreinforced and three reinforced with different technologies, through test results obtained from previous experimental campaigns on full-scale infilled frames. Two of these calibrated infill models were implemented within a FEM model of an ideal existing reinforced concrete building, and through non-linear analyses, the seismic classification according to Italian regulations was performed. Specifically, the case study building has a regular floor plan with 4 bays in one direction and 2 in the orthogonal for a total of 6 floors. The influence of the different proposed infills was presented through a comparison of the seismic classification, the Expected Annual Loss, and the main failure mechanisms at the Ultimate Limit State of the structure.

The main results are listed below.

- Infill panels strongly influenced the overall behavior of a reinforced concrete frame building under seismic actions.
- Appropriate nonlinear modeling of the infills allows for consideration of the effective resistance In-Plane but also in the Out-of-Plane.
- OOP reinforcement is useful for increasing the seismic rating of a building by more than one class, taking into account in the limit states the OOP failure and shear resistance of the columns.

ACKNOWLEDGMENTS

Special thanks are due to the Italian Department of Civil Protection and ReLUIIS, which funded this study in the framework of the ReLUIIS-DPC Project 2022-2024 – Work Package 10 Task 1.2: "Non-structural masonry".

REFERENCES

- [1] G. M. Calvi and D. Bolognini, *Seismic response of reinforced concrete frames infilled with weakly reinforced masonry panels*. *J. Earthq. Eng.*, vol. 5, no. 2, pp. 153–185, Apr. 2001, doi: 10.1080/13632460109350390.
- [2] M. Donà, M. Minotto, E. Saler, G. Tecchio, and F. da Porto, *Combined in-plane and out-of-plane seismic effects on masonry infills in RC frames*. *Int. J. Earthq. Eng.*, vol. 34, pp. 157–173, 2017.
- [3] M. Donà, M. Minotto, E. Bernardi, E. Saler, N. Verlato, and F. da Porto, *Macro-Modelling of combined in-plane and out-of-plane seismic response of thin strengthened masonry infills*. *Proceedings of the 7th International Conference on Computational*

- Methods in Structural Dynamics and Earthquake Engineering (COMPDYN 2015)*, Crete, Greece: Institute of Structural Analysis and Antiseismic Research School of Civil Engineering National Technical University of Athens (NTUA) Greece, 2019, pp. 2449–2463. doi: 10.7712/120119.7087.18838.
- [4] A. Furtado, H. Rodrigues, A. Arêde, and H. Varum, *Out-of-plane behavior of masonry infilled RC frames based on the experimental tests available: A systematic review*. *Constr. Build. Mater.*, vol. 168, pp. 831–848, Apr. 2018, doi: 10.1016/j.conbuildmat.2018.02.129.
- [5] P. Ricci, M. Di Domenico, and G. M. Verderame, *Experimental assessment of the in-plane/out-of-plane interaction in unreinforced masonry infill walls*. *Eng. Struct.*, vol. 173, pp. 960–978, Oct. 2018, doi: 10.1016/j.engstruct.2018.07.033.
- [6] A. Rossi, P. Morandi, and G. Magenes, *A novel approach for the evaluation of the economical losses due to seismic actions on RC buildings with masonry infills*. *Soil Dyn. Earthq. Eng.*, vol. 145, p. 106722, Jun. 2021, doi: 10.1016/j.soildyn.2021.106722.
- [7] M. Minotto, N. Verlato, M. Donà, and F. da Porto, *Strengthening of In-Plane and Out-of-Plane Capacity of Thin Clay Masonry Infills Using Textile- and Fiber-Reinforced Mortar*. *J. Compos. Constr.*, vol. 24, no. 6, p. 04020059, Dec. 2020, doi: 10.1061/(ASCE)CC.1943-5614.0001067.
- [8] M. T. De Risi *et al.*, *Influence of textile reinforced mortars strengthening on the in-plane/out-of-plane response of masonry infill walls in RC frames*. *Eng. Struct.*, vol. 254, 2022, doi: 10.1016/j.engstruct.2022.113887.
- [9] Federal Emergency Management Agency (FEMA), *FEMA 356 - Prestandard and commentary for the seismic rehabilitation of buildings*. 2020.
- [10] *DM n° 24 del 09-01-2020 - 'Sisma Bonus - Linee guida per la classificazione del rischio sismico delle costruzioni'*. 2020.
- [11] F. da Porto, M. Donà, N. Verlato, and G. Guidi, *Experimental Testing and Numerical Modeling of Robust Unreinforced and Reinforced Clay Masonry Infill Walls, With and Without Openings*. *Front. Built Environ.*, vol. 6, p. 591985, Dec. 2020, doi: 10.3389/fbuil.2020.591985.
- [12] CSPFEA, 'MIDAS Information Technology Co.' in MidasGen. CSPFEA. [Online]. Available: www.cspfea.net
- [13] D. C. Kent and R. Park, *Flexural Members with Confined Concrete*. *J. Struct. Div.*, vol. 97, no. 7, pp. 1969–1990, Jul. 1971, doi: 10.1061/JSDEAG.0002957.
- [14] M. Menegotto and P. E. Pinto, *Method of analysis for cyclically loaded R.C. plane frames including changes in geometry and non-elastic behaviour of elements under combined normal force and bending*. 1973, doi: 10.5169/SEALS-13741.
- [15] R. Mainstone, *Supplementary note on the stiffness and strength of infilled frames*. Garston Watford UK Build. Res. Stn., 1974.
- [16] B. Stafford Smith, *Methods for predicting the lateral stiffness and strength of multi-storey infilled frames*. *Build. Sci.*, vol. 2, no. 3, pp. 247–257, Jan. 1967, doi: 10.1016/0007-3628(67)90027-8.
- [17] M. Papia, L. Cavaleri, and M. Fossetti, *Infilled frames: Developments in the evaluation of the stiffening effect of infills*. *Struct. Eng. Mech.*, vol. 16, pp. 675–693, Dec. 2003, doi: 10.12989/sem.2003.16.6.675.
- [18] M. Donà, M. Minotto, N. Verlato, and F. da Porto, *A new macro-model to analyse the combined in-plane/out-of-plane behaviour of unreinforced and strengthened infill walls*. *Eng. Struct.*, vol. 250, p. 113487, Jan. 2022, doi: 10.1016/j.engstruct.2021.113487.
- [19] *Aggiornamento delle «Norme tecniche per le costruzioni»*. 2018.

- [20] *Istruzioni per l'applicazione dell'«Aggiornamento delle “Norme tecniche per le costruzioni”» di cui al decreto ministeriale 17 gennaio 2018.* 2019.
- [21] *Eurocode 6: Design of masonry structures.* 2015.
- [22] S. Hak, P. Morandi, and G. Magenes, *Damage Control of Masonry Infills in Seismic Design.* 2013.